

## A Study on the Stability of the Borehole in Shale, in Extended-reach Drilling

Baohua Yu<sup>1</sup>, Chuanliang Yan<sup>1</sup>, Deli Gao<sup>1,2</sup> and Jinxiang Li<sup>3</sup>

**Abstract:** Shale is easy to hydrate and often causes a collapse of the borehole during drilling, especially in drilling extended-reach wells (ERW). In order to solve the problem of collapse of the shale, the changes in the mechanical properties of shale, as affected by hydration and water absorption, are studied in this paper, through experiments. The relationships between the mechanical properties of shale and the water content are established. The borehole-stability models, which couple chemistry and mechanics are established, by considering the anisotropy of swelling, based on the experimental results. The stability of shale in the borehole is analyzed to obtain the temporal and spatial variations of the mechanical properties of shale and its stress state. Under the action of the drilling fluid, the hydration softens the shale formation, and hence the strength and stiffness of shale decrease with the increase of the openhole time and the Poisson's ratio increases with the increase of drilling time. The shale will swell, and produce the swelling strain after drilling. All these will lead to the change of the maximum tangential stress, from the wall of the borehole into the formation. The collapse pressure of shale reduces in the short time of drilling, and then increases sharply. After several days, the collapse pressure will no longer change. The present results provide a reference for studying the collapse period due to the hydration of shale in ERW drilling.

**Keywords:** ERW; shale; hydration; chemistry-mechanics coupling; anisotropy swell; borehole stability; collapse pressure

### 1 Introduction

Borehole stability is not only a pure rock mechanics problem, but also the problem of interaction between the drilling fluid and the shale while drilling fluid is a more

---

<sup>1</sup> Key Laboratory of Petroleum Engineering in the Ministry of Education, China University of Petroleum, Beijing 102249, China

<sup>2</sup> Corresponding author: Deli GAO E-mail: gaodeli@cup.edu.cn ; yubaohua73@126.com

<sup>3</sup> CNOOC Uganda Limited Beijing, China

important influencing factor (Mody, et al, 1993). Therefore, when studying the stability of a borehole in a shale-formation, the influence of the hydration of the shale on its mechanical properties must be considered. Before the 1990s, the emphasis was mainly on experimental studies of the behavior of shale. Chenevert (1970) studied how the mechanical properties of shale change after hydration. The results showed that the hydration would decrease the strength of shale. After the 1990s, the quantitative studies began to emerge. Yew (1990) and Huang (1995) combined the hydration effects on shale, quantitatively into a stress analysis model based on a thermoelasticity theory. Their method attributes all mechanical property changes in the rock, to changes in the total content of water. Considering shale as a semipermeable membrane, Hale (1993), Deng (2003) and Zhang (2009) introduced the concept of equivalent pore pressure to study the interaction of shale and the water based drilling fluid. Ghassemi and Tao (2009) proposed a linear chemistrythermo-poroelasticity coupling model, which considers the influence of temperature and chemical potential. Wang and Zhou (2012a, 2012b) built a fluid-solid-chemistry coupling model to study borehole stability, in which they considered the electrochemical potential, and the fluid flow caused by ion diffusion and its influence on solid deformation.

At present, all borehole stability models consider the effect of the coupling of chemistry and mechanics as an isotropic phenomenon, and the models are used in a vertical well. As such, these models are not suitable for ERW. Using a poroelasticity theory, a borehole stability model based on the coupling of chemistry and mechanics which can be used in ERW is presented in this paper. The present model is built according to the experimental results on the hydration of shale. In the present model, the influences of the anisotropic swelling caused by the hydration of shale are taken into consideration. Using the present model stability of the borehole and the variation of the collapse pressure are analyzed.

## 2 The Hydration of Shale, and Its Effect on Mechanical Properties of Shale

### 2.1 Experimental study on the water absorption of shale

The free water and ion would penetrate into shale, under the driving force of a pressure difference and a chemical potential difference between the drilling fluid and pore fluid after a well is drilled open(Eric, 2003). According to the conservation of mass, the water diffusion equations can be established.

Supposing that  $q$  is the mass flow rate of water diffusion,  $w(r,t)$  is weight percentage of water diffusion at the time  $t$  and distance  $r$  away from well axis, according

to conservation of mass requirement, the following equation can be established:

$$\nabla q = \frac{\partial w}{\partial t} \quad (1)$$

We hypothesise that,

$$q = C_f \nabla w \quad (2)$$

where,  $\nabla$  is the gradient operator;  $C_f$  is the coefficient of water diffusion.

According to the equations above, an equation for the diffusion of water can be established in a cylindrical-polar coordinate system as follows:

$$C_f \frac{1}{r} \frac{\partial}{\partial r} \left( r \frac{\partial w}{\partial r} \right) = \frac{\partial w}{\partial t} \quad (3)$$

The boundary conditions are:

$$\begin{cases} w = w_s & r = R_a \\ w = w_0 & r = \infty \end{cases} \quad (4)$$

Where,  $R_a$  is the borehole radius;  $w_s$  is the saturated water content of shale;  $w_0$  is the original water content of shale.

Thus, the water content of shale around the borehole can be written as follow.

$$w(r,t) = w_0 + (w_s - w_0) \left[ 1 + \int_0^\alpha e^{-C_f \cdot \zeta^2 \cdot t} \frac{J_0(\zeta r) Y_0(\zeta a) - Y_0(\zeta r) J_0(\zeta a)}{J_0^2(\zeta a) + Y_0^2(\zeta a)} \cdot \frac{d\zeta}{\zeta} \right] \quad (5)$$

Where,  $J_0()$  and  $Y_0()$  are zero order Bessel functions of group one and two, respectively

According to the above equation, the water content at anytime and anywhere near the borehole can be obtained through finite difference method or infinite integral method.

Owing to the direct contact of drilling fluid and shale around the borehole, the free water of drilling fluid diffuses into the shale under different kinds of physical and chemical driving forces. The minerals of shale absorb water and produce the swelling strain, which leads to a hydration stress (Fontoura, et al., 2002). In order to calculate the hydration stress, the coefficient of water absorption and diffusion and the swelling ratio must be determined first (Chenevert, et al, 1998).

The water diffusion character of shale is tested using the experimental equipment of the rock mechanics laboratory in China University of Petroleum (Deng, et al, 2002). All the core samples used in this paper were collected from M oilfield. The fluid which comes in to contact with the shale in experiments is the KCL/PHPA/GLYDRIL drilling fluid used in M oilfield. The experimental confining pressure is 30MPa, and the differential pressure of the fluid is 8MPa. The core is taken out after 50 hours and cut into pieces to test the water content of each piece. The results are shown in the Figure 1. Substituting those data into equation 5, the coefficient of water absorption and diffusion of the shale can be obtained as  $C_f = 0.0527$ .

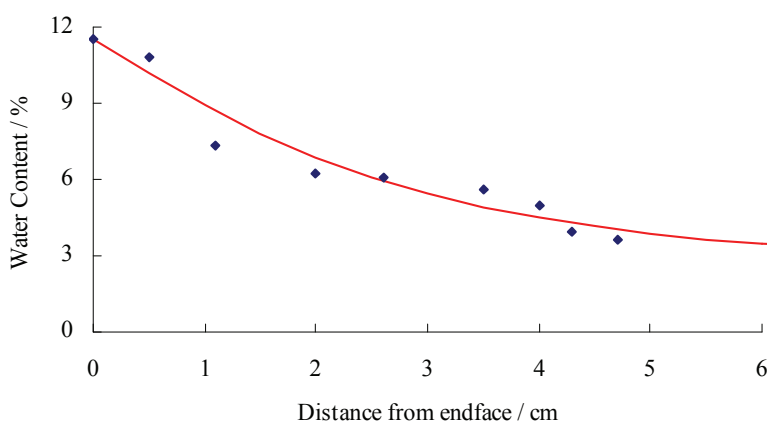


Figure 1: Experimental results of water diffusion in shale

## 2.2 Experimental Study on the Variation of Mechanical Properties of Shale

After water absorption, shale would produce a swelling strain, which leads to a hydration stress. In order to calculate the hydration stress, the relation between water absorption and the swelling ratio must be presented first through experiments. The experimental equipment is similar to that used by Yew and Chenevert (1990). The experimental results are shown in figure 2.

The experimental results show that the swelling in the direction which is perpendicular to the deposition surface is much larger than that in the parallel direction, which might be due to the differences in drainage and stress conditions in different directions in the process of sedimentation and diagenesis (Weaver, 1989). The relationship between the swelling strain and the water content is as follows:

$$\varepsilon_v = -244.35(\Delta W)^3 + 21.2(\Delta W)^2 + 0.41\Delta W \quad (6)$$

$$\epsilon_h = -75.75(\Delta W)^3 + 6.57(\Delta W)^2 + 0.13\Delta W \quad (7)$$

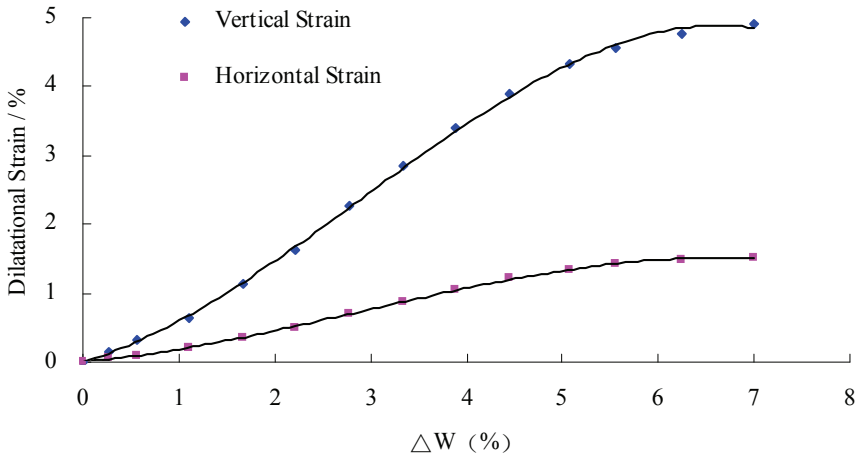


Figure 2: Experimental results of shale swelling

After water absorption, shale would be softened, and its stiffness and strength characteristics would change with the water content (Lu, et al, 2012). In order to evaluate the stability of a borehole after the hydration of shale, the elasticity and strength parameters of shale must be studied. In order to ensure the uniformity of the cores used in experiment, velocities of the compressive acoustic wave of cores are tested under the same conditions. Only the cores whose velocity is close are chosen. The cores are soaked in the KCL/PHPA/GLYDRIL drilling fluid, at the temperature of 60°C.

In order to determine cohesive force and internal friction angle, two pieces of cores at the same immersing time and under the different confining pressure should be tested. Experimental equipment from the TerraTek company was adopted to test the mechanical properties of shale under triaxial compressive stresses. In the experiments 18 cores whose immersing time is different are tested. The experimental results are shown in the table 1.

The effect of the water content on elastic modulus of shale is shown in figure 3. The elastic modulus of shale reduces with an increase in water content. The reduction rate at the beginning is sharp and then become slow. The equation of the relationship between the elastic modulus and water content can be obtained as:

$$E = 3.93 \times 10^3 e^{-4.5\sqrt{\Delta w}} \quad (8)$$

Where,  $E$  is the elastic modulus of shale; and  $\Delta W$  is the water content increment in shale.

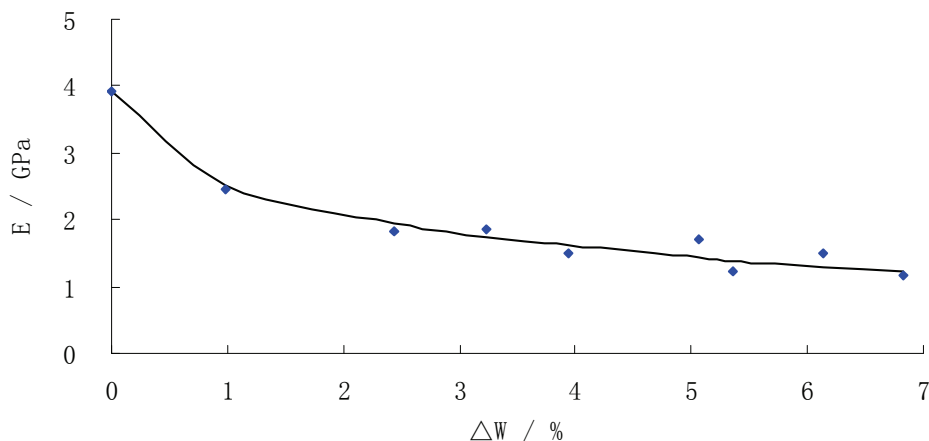


Figure 3: Variation of the elastic modulus of shale, with water content

The effect of water content on Poisson's ratio is shown in Figure 4. The Poisson's ratio increases with an increase in water content. The equation of the relationship between the Poisson's ratio of shale and its water content can be approximated as:

$$\mu = 0.28 + 1.42\Delta W \quad (9)$$

where,  $\mu$  is Poisson's ratio.

The effect of water content on UCS is shown in Figure 5. UCS reduces with an increase in water content. The relationship between the UCS and water content can be approximated as:

$$UCS = 11.83 - 105.87\Delta W \quad (10)$$

where, UCS is the unconfined compressive strength of shale.

Borehole shear failure obeys the Mohr-Coulomb strength criterion. When the Mohr's circle is expressed by maximum and minimum effective principal stresses the Mohr-Coulomb strength criterion can be expressed by the principal stress (Chen, et al, 2008):

$$\sigma_1 = \sigma_3 ctg^2 \left( 45^\circ - \frac{\phi}{2} \right) + 2C ctg \left( 45^\circ - \frac{\phi}{2} \right) \quad (11)$$

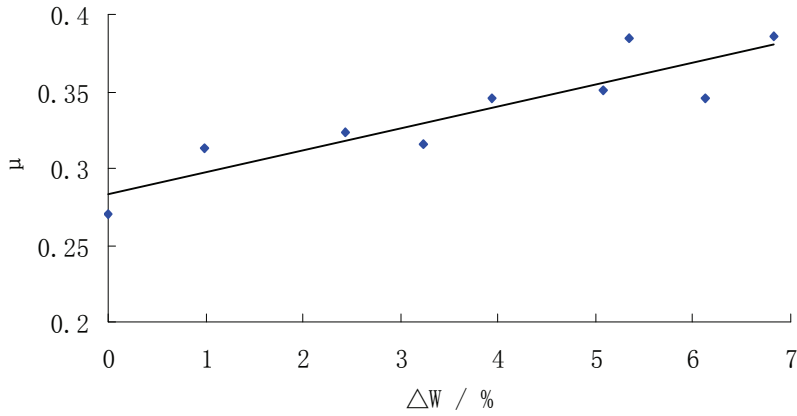


Figure 4: Relationship Between the Poisson's ratio of Shale and its water content

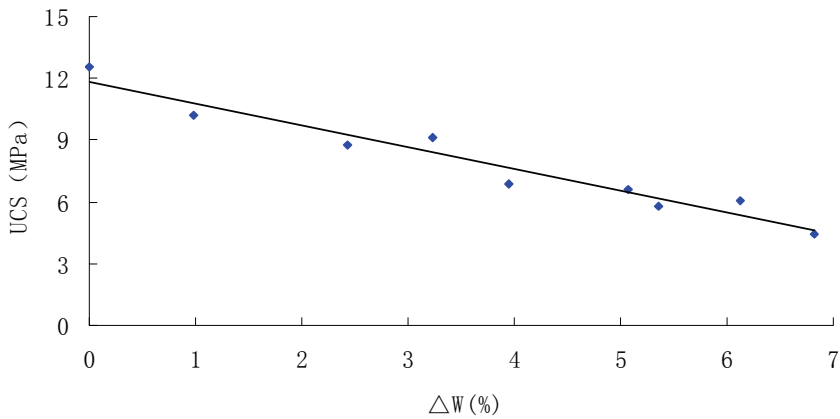


Figure 5: Relationship Between the UCS of Shale and its water content

Where,  $\sigma_1$  and  $\sigma_3$  are the maximum and minimum effective principal stresses respectively;  $C$  is the cohesive strength; and  $\varphi$  is internal friction angle.

The effect of water content on the cohesive force is shown in Figure 6. The cohesive force reduces with an increase in water content. The relationship between the cohesive force and water content can be approximated as:

$$C = 3.13 - 16.35\Delta W \quad (12)$$

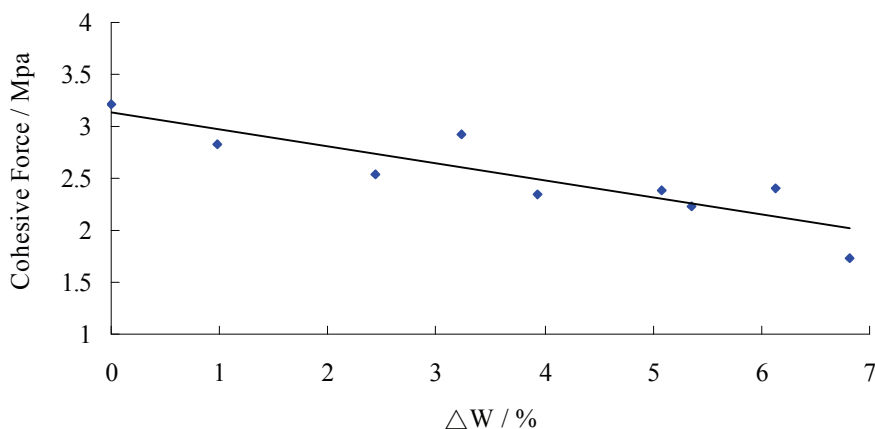


Figure 6: Relationship of cohesive force and water content

The effect of water content on the internal friction angle is shown in Figure 7. The relationship between the internal friction angle and the water content can be approximated as:

$$\phi = 36.07 - 351.29\Delta W \quad (13)$$

### 3 A Model for the Stability of the Borehole in ERW, Including the Effect of Hydration of Shale

The stability of boreholes in inclined wells has a remarkable difference from the stability in vertical wells owing primarily to the inclination. The stability of the borehole is related not only to the borehole trajectory (well inclination, azimuth), but also the orientation of the in-situ stresses. Combined with an appropriate failure model research on the mechanical stability of boreholes in deviated wells should be based on the borehole circumferential stress field. Then a reasonable mechanical



Table 1: Experiment results of cores immersing in the drilling fluid

Uniaxial	Immersing time (h)	0	2	6	12	24	36	48	96	192
	Water content increment $\Delta W$ (%)	0	0.98	2.43	3.24	3.94	5.07	5.35	6.13	6.82
	Strength (MPa)	12.5	10.24	8.76	9.11	6.88	6.64	5.80	6.05	4.47
	Poisson's ratio	0.27	0.31	0.32	0.32	0.35	0.35	0.38	0.35	0.39
	Elastic modulus (GPa)	3.93	2.44	1.83	1.86	1.49	1.70	1.24	1.50	1.16
Confining Pressure: 10MPa	Immersing time (h)	0	2	6	12	24	36	48	96	192
	Water content Increment $\Delta W$ (%)	0	0.91	2.08	3.73	4.05	5.22	5.39	6.27	7.01
	Strength (MPa)	50.4	43.1	38.7	33.5	28.4	26.1	22.8	21.9	21.1
	Poisson's ratio	0.24	0.31	0.32	0.32	0.35	0.35	0.38	0.35	0.39
	Elastic modulus (GPa)	4.83	2.44	1.83	1.86	1.49	1.70	1.24	1.50	1.16

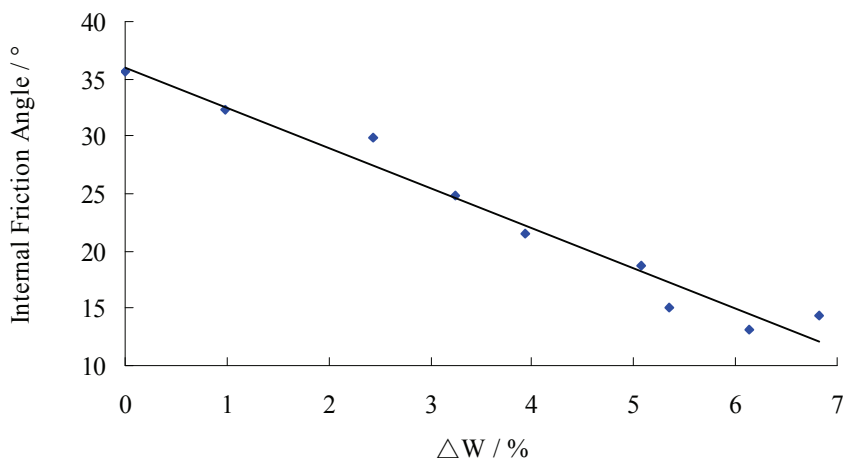


Figure 7: Relationship between the internal friction angle and the water content

model can be established, so as to determine the safe mud density of deviated wells (Jin and Chen, et al., 1999).

A deviated well is drilled through shale formation as shown in Figure 8. The following coordinate system should be established first, before model is described:

- 1) Coordinate system  $[X \ Y \ Z]$  for geomagnetic coordinate system;  $X$  corresponds to the east direction;  $Y$  corresponds to the north direction;  $Z$  corresponds to the sky.
- 2) For borehole coordinate system  $[x \ y \ z]$ ,  $\beta_b$  is deviation angle;  $\alpha_b$  is azimuth angle. The transformation relationship between borehole coordinates and geomagnetic coordinates is shown in Figure 8A.
- 3) For the in-situ stress coordinate system  $[X_s \ Y_s \ Z_s]$ ,  $X_s, Y_s, Z_s$  respectively corresponds to three principal stresses  $\sigma_H, \sigma_h, \sigma_v$ . The  $\sigma_H$  and  $\sigma_h$  are in the horizontal plane, and the azimuth of maximum horizontal principal stress is  $\omega$ . The transformation relationship between the in-situ stress coordinates and the geomagnetic coordinates is shown in Figure 8B.
- 4) For the coordinate system  $[s \ t \ n]$  in the deposition plane, the tendency of deposition plane is  $\alpha_r$  and the inclination angle is  $\beta_r$ . The transformation relationship between deposition plane coordinates and geomagnetic coordinates is shown in Figure 8C.

The formation is equilibrated in its in-situ stress-state, before drilling. In in-situ

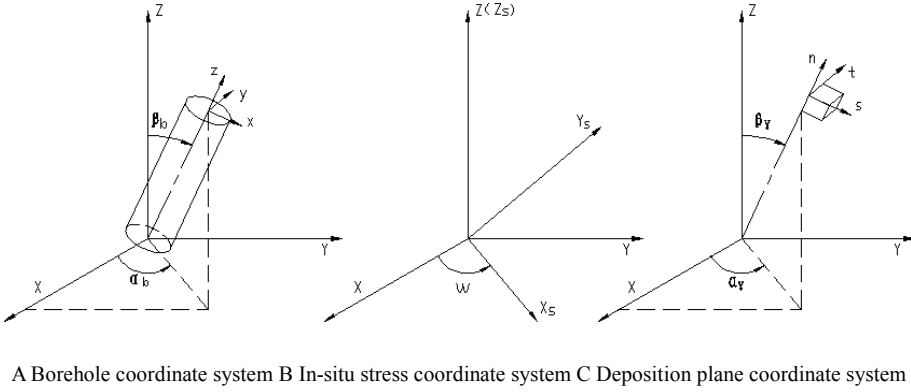


Figure 8: Correspondence of local coordinate system and the geomagnetic coordinate system

stress coordinate system, the formation stress state is as follows:

$$[\sigma] = \begin{bmatrix} \sigma_H & 0 & 0 \\ 0 & \sigma_h & 0 \\ 0 & 0 & \sigma_v \end{bmatrix} \quad (14)$$

The analysis of borehole stress and deformation is based on the borehole coordinate system, so the borehole stability analysis model is established according to borehole coordinate system. For an inclined well, the borehole coordinate system and the in-situ stress coordinate system do not coincide, so that the stress state of the in-situ stress coordinate system should be transformed into that of the borehole coordinate system. On the basis of the coordinate transformation relation shown in Figure 8, the transformation matrix between in-situ stresses coordinate system and borehole coordinate system is as follows:

$$[L] = \begin{bmatrix} \cos \beta_b \cos \alpha & \cos \beta_b \sin \alpha & -\sin \beta_b \\ -\sin \alpha & \cos \alpha & 0 \\ \sin \beta_b \cos \alpha & \sin \beta_b \sin \alpha & \cos \beta_b \end{bmatrix} \quad (15)$$

Where,  $\alpha = \omega - \alpha_b$ .

According to the transformation relationship of stress tensor in different coordinate

systems, the initial stress state in borehole coordinate system is as follows:

$$\begin{bmatrix} \sigma_{xx} & \sigma_{xy} & \sigma_{xz} \\ \sigma_{yx} & \sigma_{yy} & \sigma_{yz} \\ \sigma_{zx} & \sigma_{zy} & \sigma_{zz} \end{bmatrix} = [L] \begin{bmatrix} \sigma_H & & \\ & \sigma_h & \\ & & \sigma_z \end{bmatrix} [L]^T \quad (16)$$

The formation of borehole is replaced by the mud with fluid column pressure  $p_w$  after drilling. The original balance of the formation surrounding the borehole is broken. Under the mud column pressure, a new balance will be built in the formation surrounding the borehole. Without regard to the instantaneous dynamic effect when the borehole is drilled, in borehole Cartesian coordinate systems, the stress balance equation of formation surrounding the borehole is as follows (Xu, et al, 1998):

$$\sigma_{ij,j} + f_i = 0 \quad (17)$$

Where,  $\sigma_{ij}$  is the total stress tensor,  $f_i$  is the volume force of rock.

The borehole stress boundary condition is as follows (Deng, et al, 1997):

$$\sigma_r = P_w \quad (18)$$

Where,  $\sigma_r$  is the borehole radial stress,  $P_w$  is the drilling fluid column pressure.

Under condition of small deformation, the formation strain components and displacement components shall meet the following geometric equation (Xu, et al, 1998):

$$\varepsilon_{ij} = \frac{1}{2} (u_{i,j} + u_{j,i}) \quad (19)$$

Where,  $\varepsilon_{ij}$  is total strain tensor;  $u_i$  is the displacement component.

As the main deformation and destruction of rock skeleton is controlled by effective stress, on the basis of Biot's effective stress theory a equation can be established:

$$\sigma'_{ij} = \sigma_{ij} - \alpha P_p \delta_{ij} \quad (20)$$

Where,  $\sigma_{ij}$  is the total stress tensor,  $\sigma'_{ij}$  is the effective stress tensor,  $\alpha$  is the effective stress coefficient,  $\delta_{ij}$  is Kronecker symbol,  $P_p$  is pore pressure, Owing to the extremely low permeability of shale, the fluid flow is controlled by the effect of diffusion in the rock. The pore pressure in the process of diffusion is constant in this paper.

Stress-strain constitutive equation is the basis of research on borehole deformation and failure law. The effective stress-strain constitutive relationship is expressed in incremental form under the condition of hydration strain:

$$d\sigma' = D_T (d\varepsilon - d\varepsilon_p - d\varepsilon_0) \quad (21)$$

Where,  $D_T$  is the rock constitutive matrix,  $d\varepsilon$  is the total strain vector increment of rock matrix.  $d\varepsilon_p$  is rock skeleton strain vector increment caused by changes of pore pressure (Charlez, 1997):

$$d\varepsilon_p = -m^T \frac{dp}{3K_s} \quad (22)$$

Where,  $K_s$  is the average bulk modulus of rock matrix.  $m = [\alpha \ \alpha \ \alpha \ 0 \ 0 \ 0]$ ,  $\alpha$  is the effective stress coefficient.

$$d\varepsilon_0 = [d\varepsilon_h \ d\varepsilon_h \ d\varepsilon_v \ 0 \ 0 \ 0] \quad (23)$$

Where,  $d\varepsilon_h$  and  $d\varepsilon_v$  are swelling strain parallel to the plane and perpendicular to the plane respectively.

The formation is assumed to be a homogeneous and isotropic elastic material. The formation constitutive matrix  $D_T$  can be made of elastic modulus  $E$  and Poisson ratio  $\nu$ .  $E$  and  $\nu$  can change with borehole drilling time and formation water content and be determined by the above experiments. Hence, the elastic constitutive matrix of the rock can be expressed as follows:

$$D_T = \frac{E}{(1+\nu)(1-2\nu)} \begin{bmatrix} 1-\nu & \nu & \nu & 0 & 0 & 0 \\ & 1-\nu & \nu & 0 & 0 & 0 \\ & & 1-\nu & 0 & 0 & 0 \\ & & & \frac{1-2\nu}{2} & 0 & 0 \\ & & & & \frac{1-2\nu}{2} & 0 \\ \text{Symmetric} & & & & & \frac{1-2\nu}{2} \end{bmatrix} \quad (24)$$

Where,  $E = E(t, w)$ ,  $\nu = \nu(t, w)$ .

The elastic matrix above is defined in the local coordinate system of deposition plane, but the borehole stress and deformation of borehole stability analysis are based on borehole coordinates. Therefore the elastic matrix of deposition plane local coordinate system needs to be transformed into that of borehole coordinate system.

On the basis of transformation relationship shown in Figure 8, the transformation relationship between the deposition plane coordinate system and borehole coordinate system is as follows:

$$[T] = \begin{bmatrix} \cos \beta \cos \alpha & \cos \beta \sin \alpha & -\sin \beta \\ -\sin \alpha & \cos \alpha & 0 \\ \sin \beta \cos \alpha & \sin \beta \sin \alpha & \cos \beta \end{bmatrix} \quad (25)$$

Where,  $\alpha = \alpha_r - \alpha_b$ ,  $\beta = \beta_r - \beta_b$ .

From the stress tensor transformation law in different coordinate system, the stress tensor in deposition plane coordinates is as follows:

$$\begin{bmatrix} \sigma_{xx} & \sigma_{xy} & \sigma_{xz} \\ \sigma_{yx} & \sigma_{yy} & \sigma_{yz} \\ \sigma_{zx} & \sigma_{zy} & \sigma_{zz} \end{bmatrix} = [T] \begin{bmatrix} \sigma_{ss} & \sigma_{st} & \sigma_{sn} \\ \sigma_{ts} & \sigma_{tt} & \sigma_{tn} \\ \sigma_{ns} & \sigma_{nt} & \sigma_{nn} \end{bmatrix} [T]^T \quad (26)$$

The above equation can be written in the form of stress vector:

$$[\sigma]_r = [q][\sigma]_b \quad (27)$$

Where,  $[\sigma]_r$ ,  $[\sigma]_b$  are stress tensor in deposition plane coordinate system and borehole coordinate system respectively;  $[q]$  is a  $6 \times 6$  matrix, whose component is determined by the expansion form of equation (27).

Similarly, the strain vector in the bedding plane coordinate system is as follows:

$$[\varepsilon]_r = [q][\varepsilon]_b \quad (28)$$

The stress and strain vectors are written in the form of increments:

$$[d\sigma]_r = [q][d\sigma]_b, \quad [d\varepsilon]_r = [q][d\varepsilon]_b \quad (29)$$

The equation (29) is plugged into equation (21), then the elastic matrix D in borehole coordinate system can be obtained:

$$D = qD_Tq \quad (30)$$

According to above governing equations, the borehole circumferential stress distribution and its variation with the drilling time of the inclined well are obtained under drilling fluid of certain density. Combined with Mohr-Coulomb failure criterion, the variation of the collapse pressure can be obtained, using the finite element method.

#### 4 The time dependent character of borehole collapsing pressure

Based on the present analytical model for the stability of the borehole, and the experimental results, the variations of mechanical properties of shale around the borehole and their effects on the borehole stability of the M oilfield with the open hole time are studied. The calculated parameters are as follows: well depth  $H = 2200m$ , formation initial water content  $W_0 = 3.5\%$ , saturation water content  $W_s = 12\%$ , borehole radius  $R_a = 10.8cm$ , equivalent in-situ stress density  $\sigma_H = 1.93g/cm^3$ ,  $\sigma_h = 1.57g/cm^3$ ,  $\sigma_v = 2.10g/cm^3$ , maximum horizontal in-situ stress azimuth  $\omega = 35^\circ$ , stratigraphic dip  $\beta_r = 0^\circ$ , the other parameters are obtained by experimental results.

##### 4.1 Nature of Variation of the initial collapse pressure of the borehole

The variation of the collapse pressure of the deviated borehole, versus the inclination and azimuth is presented in Figure 9, when the borehole is just opened. The circular direction is the azimuth and the radial direction is the inclination. The calculated results show that the collapse pressure of the deviated borehole ranges from  $1.24g/cm^3$  to  $1.36g/cm^3$ . When the inclination is small, the collapse pressure in any direction is low and it rises with increasing inclination. The extended-reach drilling inclination is usually higher than  $45^\circ$  and the collapse pressure is obviously higher than that of the vertical well, the risk of instability of the borehole is increased. With the same inclination, the collapse pressure in the maximum horizontal in-situ stress direction is the highest and the risk is the highest, the collapse pressure in the minimum horizontal in-situ stress direction is the lowest.

##### 4.2 The Variation of the mechanical properties of the formation around the borehole

Figure10 illustrates the variation of water content in shale around borehole with different open hole times. The calculated results show that the water content of the shale at the borehole wall reaches a saturated state quickly after the borehole is opened; in the same time, the water content of shale would decrease with the increase of distance from borehole axis and the decreasing rate is the highest near the borehole wall. Thus a hydrated area would develop in shale formation around the borehole. When the distance from hole axis exceeds 25cm, the formation water content almost no longer changes no matter how much the time increases and the water content approaches initial water content; in the hydrated area, when the distance is constant, the longer the time, the more the shale water content.

The variations of the uniaxial compressive strength (UCS), the elastic modulus and the Poisson's ratio of the shale around borehole are presented in Fig.11, Fig.12 and

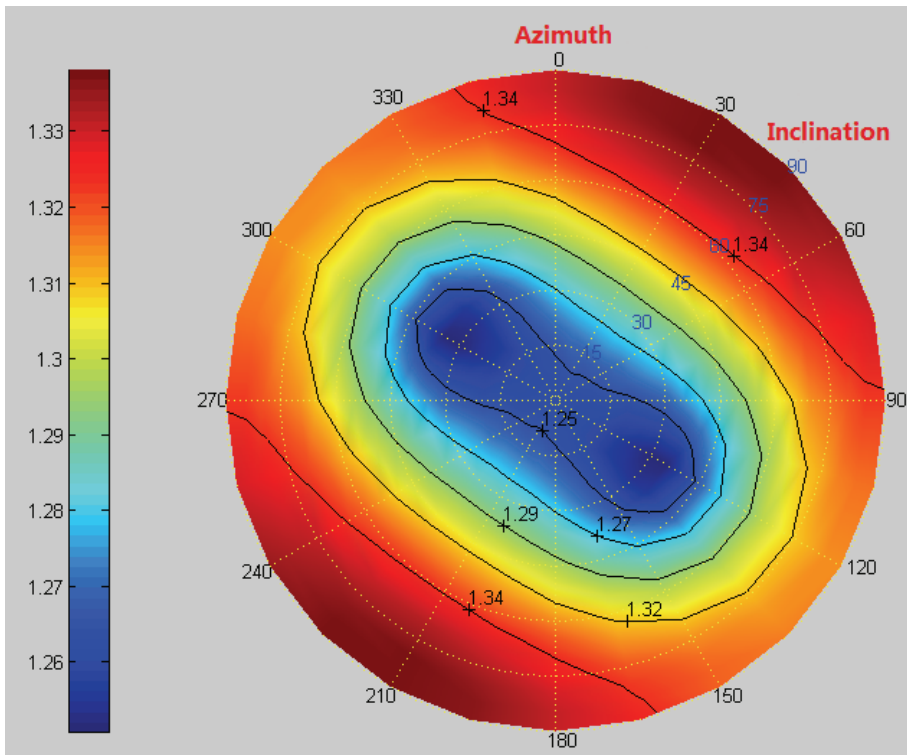


Figure 9: The distribution character of deviated borehole collapsing pressure versus well track

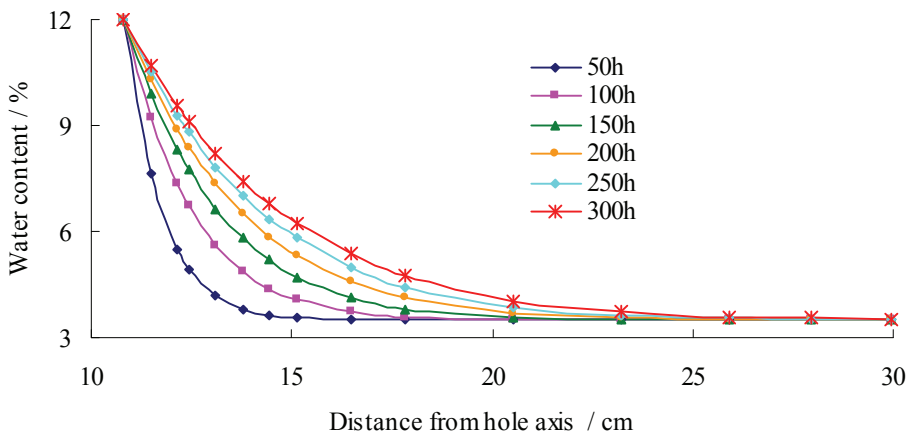


Figure 10: Water content distribution in the shale around borehole



Fig.13, respectively. The results show that the variations of uniaxial compressive strength and elastic modulus are similar. When the hole is opened, the uniaxial compressive strength and elastic modulus would decrease as the time increases. When the time is constant, the uniaxial compressive strength and elastic modulus would increase as the distance from borehole axis increases and the rate of increase near the well wall is the highest. The Poisson's ratio would increase as the open hole time increases and decreases as the distance from hole axis increases.

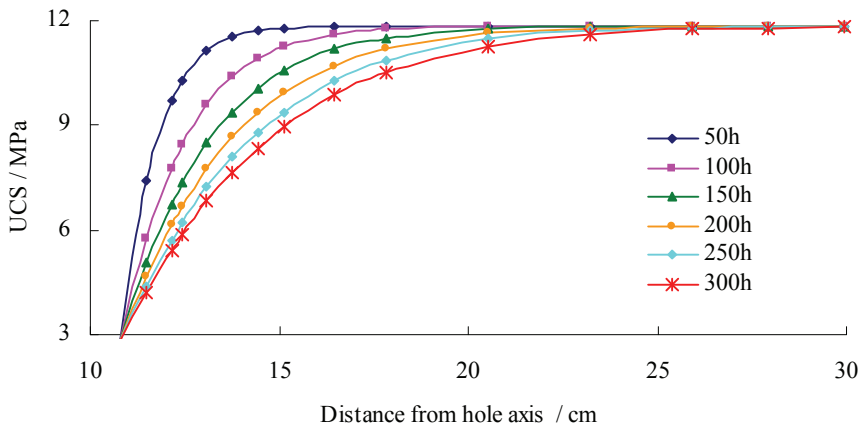


Figure 11: Variation of the UCS of the shale near the borehole

#### 4.3 Time dependent character of the borehole collapse pressure

Figure 14 illustrates the variations of the stresses around the borehole, for different values of the open hole time in the maximum horizontal in-situ stress directions. The hydration would soften the formation and decrease the tangential stress near borehole wall. Although the swelling strain caused by water absorption would increase the stress, the influence of shale softness caused by the decreasing formation rigidity on the stress is more important (Deng, et al, 2003). Meanwhile, the maximum tangential stress is not at borehole wall, it is at a certain distance from borehole wall, and its location moves into formation as the time increases. The radial stress at a the distance would decrease as the hole opening time increases and leads to borehole instability. Thus the borehole instability is not at the well wall, but it is in the formation. It is reflected by a periodic collapsing character and produces a great volume of cavings which is harmful for the drilling.

Figure 15 illustrates the variation of the collapse pressure with the open hole time. The calculated results show that the borehole collapse pressure is low in a short

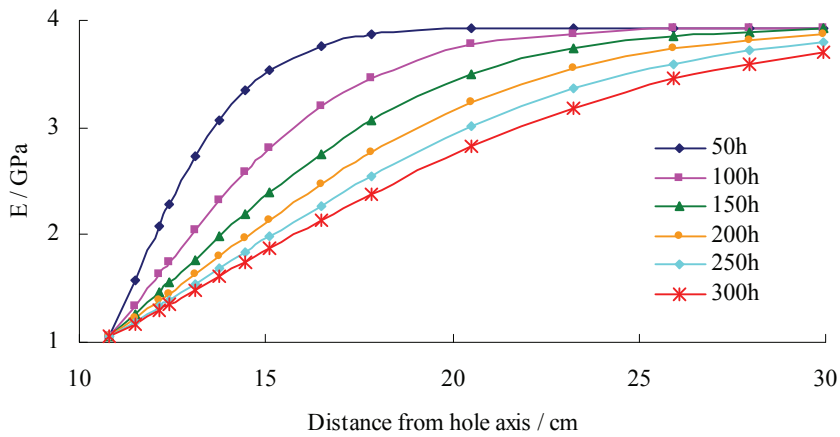


Figure 12: Variation of the Elastic modulus of the shale, near the borehole

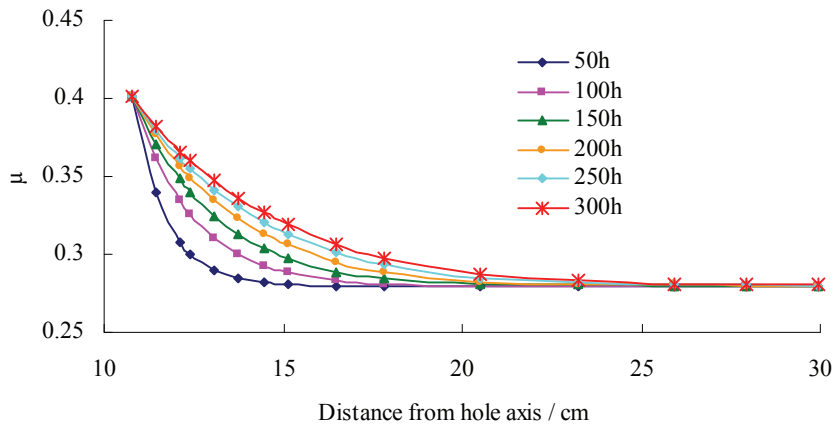


Figure 13: Variation of the Poisson's ratio of the shale, near the borehole

time after borehole opening due to shale hydration and reaches its lowest value at about 10 hours. However, after that the collapse pressure would increase rapidly and reach the initial value after about 40 hours. Then the rate of increase of the collapse pressure would decrease, and reach  $1.31\text{g/cm}^3$  after about 4 days. At last, the collapse pressure would increase linearly and the rate of increase is very low. After the hole is opened for 10 days, the borehole collapse pressure would be fixed at about  $1.35\text{g/cm}^3$  and no longer changes. According to the calculation, after the borehole opening, gradually increasing the drilling fluid density to  $1.35\text{g/cm}^3$  is of more benefit for longtime borehole stability.

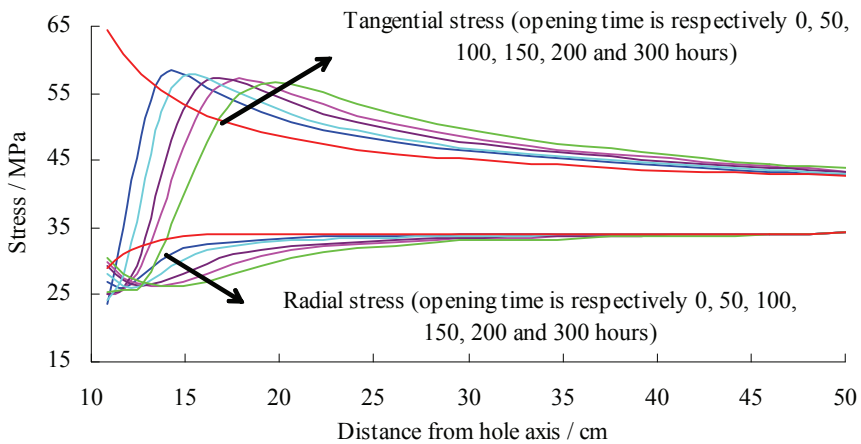


Figure 14: The influence of shale hydration on the stress distributions near the borehole

## 5 Conclusions

1. The swelling of the shale in the direction perpendicular to the deposition surface is much larger than that in the parallel direction. The strength and stiffness of the shale formation decrease with the increase of the water content and the Poisson's ratio increases with the water content.
2. Due to the impact of the shale hydration, the strength and the stiffness of the circumferential formation around the well are gradually reduced with the increase of drilling time and increase with the increase of the distance away from the borehole; the Poisson's ratio increases gradually with the drilling time and decreases with the increase of the distance; the location of the max-

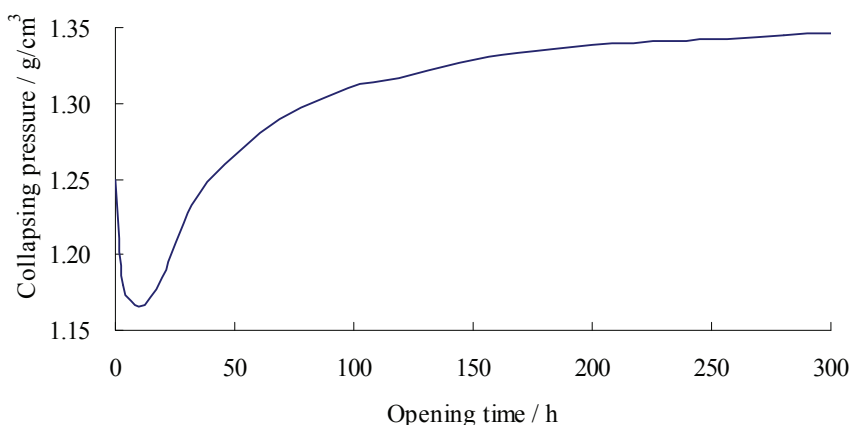


Figure 15: Variation of the Collapse Pressure, with the open hole time

imum circumferential stress around the well gradually enters into the formation so that the collapse occurs inside the formation instead of at the borehole wall; the initial steady borehole would collapse with the increase of the open hole time.

3. The collapse pressure of the shale decreases in a short time after the shale formation is drilled and is followed by a rapid increase, while the rate slows down gradually. The borehole collapse pressure is basically stable after several days of the open hole time.

**Acknowledgement:** The authors gratefully acknowledge the support of Science Fund for Creative Research Groups of the National Natural Science Foundation of China (Grant No.: 51221003) and the National Oil and Gas Major Project (Grant No. 2011ZX05009-005).

## References

- Chenevert, M.E.; Pernot, V.** (1998): Control of shale swelling pressures using inhibitive water-base muds. *SPE*, 67th SPE Annual Technical Conference and Exhibition, New Orleans, LA, 49263, pp. 27-30.
- Chenevert, M.E.** (1970): Shale Alteration by Water Adsorption. *SPE*, 2401, pp. 1141-1148.

**Chen, M.; Jin, Y.; Zhang, G.Q.** (2008): *Petroleum related rock mechanics*. Beijing: Science Press.

**Charlez, P.A.** (1997): *Rock Mechanics: Volume 2, Petroleum applications*. Paris, France : Editions Technip.

**Deng J.G.** (1997): Calculation method of mud density to control borehole closure rate. *Chinese Journal of Rock Mechanics and Engineering*, Vol. 16(6), pp. 522–528.

**Deng, J.G.; Wang, J.F.; Luo, J.S.** (2002): A new experimental method to measure diffusion coefficient of shale hydration. *Rock and Soil Mechanics*, Vol. 23, pp. 40-42.

**Deng, J.G.; Guo, D.X.; Zhou, J.L.** (2003): Mechanics-chemistry coupling calculation model of borehole stressing in shale formation and its numerical solving method. *Chinese Journal of Rock Mechanics and Engineering*, Vol.22 (Supp.1), pp. 2250-2253.

**Eric, V.O.** (2003): On the physical and chemical stability of shales. *Journal of Petroleum Science and Engineering*, Vol. 38, pp. 213-235.

**Eric, V.O.; Hale, A.H.; Mody, F.K.** (1994): Critical Parameters in modeling the chemical aspects of borehole stability in shales and in designing improved water-based shale drilling fluids. *SPE*, pp. 171-186.

**Fontoura, C.R.; Rosana, F.T.L.** (2002): Characterization of shales for drilling purposes. *SPE/ISRM*, 78218.

**Ghassemi, A.; Tao, Q.; Diek, A.** (2009): Influence of coupled chemo-poro-thermoelastic processes on pore pressure and stress distributions around a wellbore in swelling shale. *Journal of Petroleum Science and Engineering*, Vol. 67(1/2), pp. 57-64.

**Hale, A.H.; Mody, F.K.** (1993): Borehole-Stability Model To Couple the Mechanics and Chemistry of Drilling-Fluid/Shale Interactions. *Journal of Petroleum Technology*, Vol. 45(11), pp. 1093-1101.

**Hale, A.H.; Mody, F.K.; Salisbury, D.P.** (1993): The influence of chemical potential on wellbore stability. *SPE*, 23885-PA.

**Huang, R.Z.; Chen, M.; Deng, J.G.** (1995): Study on shale stability of wellbore by mechanics coupling with chemistry method. *Drilling Fluid & Completion Fluid*, Vol. 12(3), pp. 15-21, 25.

**Jin,Y.; Chen,M.; Liu, G.H.** (1999): Wellbore stability analysis of extended reach wells. *Journal of geomechanics*, Vol. 5(1), pp.4-11.

**Lu, Y.H.; Chen, M.; Jin, Y.; Teng, X.Q.; Wu, W.; Liu X.Q.** (2012): Experimental study of strength properties of deep mudstone under drilling fluid soaking. *Chinese Journal of Rock Mechanics and Engineering*, Vol. 31(7), pp. 1399-1405.

**Wang, Q.; Zhou Y.C.; Tan, Y.L.; Jiang, Z.B.** (2012a): Analysis of effect factor in shale wellbore stability. *Chinese Journal of Rock Mechanics and Engineering*, Vol. 31(1), pp. 171-179.

**Wang, Q.; Zhou, Y.C.; Wang, G.; Jiang, H.W.; Liu, Y.S.** (2012b): A fluid-solid-chemistry coupling model for shale wellbore stability. *Petroleum Exploration and Development*, Vol. 39(4), pp. 475-480.

**Weaver, C.E.** (1989): *Clays, muds, and shales*. Elsevier.

**Xu, Z.L.** (1998): *Elastic mechanics*. Beijing Higher Education Press.

**Yew, C.H.; Chenevert, M.E.** (1990): Wellbore Stress Distribution Produced by Moisture Adsorption. *SPE*, 19536.

**Zhang, L.W.; Qiu, D.H.; Cheng, Y.F.** (2009): Research on the wellbore stability model coupled mechanics and chemistry. *Journal of Shandong University: Engineering Science*, Vol. 39(3), pp. 111-114.